

## Characterization of surface layers in Zn-diffused LiNbO<sub>3</sub> waveguides by heavy ion elastic recoil detection

O. Espeso-Gil, G. García, F. Agulló-López,<sup>a)</sup> and A. Climent-Font  
*Centro de Micro-Análisis de Materiales, Univ. Autónoma de Madrid, 28049 Madrid, Spain*

T. Sajavaara  
*Accelerator Laboratory, P.O. Box 43, FIN-00014, University of Helsinki, Finland*

M. Domenech, E. Cantelar, and G. Lifante  
*Departamento de Física de Materiales, C-IV, Universidad Autónoma de Madrid, 28049 Madrid, Spain*

(Received 24 May 2002; accepted for publication 22 July 2002)

The surface layers formed in LiNbO<sub>3</sub> waveguides, fabricated by Zn diffusion from the vapor phase, have been investigated by time of flight elastic recoil detection analysis using <sup>127</sup>I ions. The key features of this technique, simultaneous profiling of all ions and a depth of analysis <1 μm, have allowed a detailed and quantitative characterization of the surface layers. The Zn diffusion into LiNbO<sub>3</sub> can be understood as a 2Li↔Zn exchange process. As a consequence, an outermost layer of several hundreds of nanometers is formed, consisting of LiNbO<sub>3</sub> and ZnNb<sub>2</sub>O<sub>6</sub> phases showing complementary profiles. A good correlation has been found between the composition profiles and the optical waveguiding behavior. After thermal annealing of the waveguides, a thinner layer containing a uniform mixture of ZnO and LiNbO<sub>3</sub> is generated followed by a transition to a graded solid solution of Zn into LiNbO<sub>3</sub>. © 2002 American Institute of Physics.  
[DOI: 10.1063/1.1506405]

Different methods are available for the fabrication of good-quality low-loss waveguides in LiNbO<sub>3</sub>. In particular, Ti diffusion, performed at 900–1100 °C, has been commercially implemented for many years for the fabrication of a variety of integrated optics devices.<sup>1</sup> Unfortunately, optical damage (photorefractive effect) severely impairs the use of these waveguides for high-power density applications such as lasers and nonlinear optical devices in the visible range. Several alternatives to Ti diffusion have been put forward and are being developed. One promising approach is Zn diffusion from the vapor phase,<sup>2</sup> from a ZnO source,<sup>3</sup> or by liquid-phase epitaxy.<sup>4</sup> In the first procedure, the diffusion temperature is much lower (550–800 °C) than that for Ti diffusion and therefore it is free of many problems derived from the high temperature processing. The Zn-doped material presents good crystallinity, transparency,<sup>5</sup> and resistance to laser damage.<sup>6</sup> At the same time, they preserve the high electrooptic coefficients<sup>7</sup> and the ferroelectric domain structure of the LiNbO<sub>3</sub> substrate.<sup>8</sup> The fabrication process involves two steps: the diffusion of Zn from the vapor phase at 500–700 °C, followed by an annealing step performed at 800–900 °C. Some laser and nonlinear optical devices have been already implemented on Zn-doped waveguides.<sup>9,10</sup> However, the physical characterization of the waveguides is still deficient. Optical experiments have suggested the formation of a multilayer structure with a thin low-index film at the surface,<sup>11</sup> although a direct experimental confirmation is lacking. In fact, the techniques used so far are either insensitive to these surface layers or not quantitative enough to provide a detailed and reliable picture.

The purpose of this work has been to apply the potential

of the time of flight elastic recoil detection analysis (TOF–ERDA) method<sup>12</sup> using heavy <sup>127</sup>I ions to determine the near-surface profiles of all relevant atom species. The main advantage of this technique is that the information for all elements is retrieved in the same experiment so that meaningful correlations can be established. Moreover, the depth range of the technique (<1000 nm) is particularly suitable for the investigation of surface layers such as those invoked to account for the optical behavior of the waveguides.

Zn-diffused waveguides were fabricated in congruent Z-cut LiNbO<sub>3</sub> substrates supplied by Crystal Technology Inc. In the first stage of the process the crystal plates were subjected to a Zn vapor atmosphere at a temperature of either 550 or 600 °C and a pressure of 560 mbar. Diffusion times were 30 and 120 min. The reactor used to perform this treatment is described elsewhere.<sup>13</sup> In a second (annealing) step, that was the same for all samples, crystals were heated in air at 900 °C for 1 h. The x-ray characterization was done with a D5000HR Bruker diffractometer (Cu K<sub>α</sub> emission line). For the optical characterization, the dark *m* lines method was used (λ = –633 nm).

The TOF–ERDA experiments were performed in the 5 MV EGP-10-II tandem accelerator in the Accelerator Laboratory at the University of Helsinki using 55 MeV <sup>127</sup>I<sup>11+</sup> as primary ions. The angle between the incident beam and sample surface was 20° and the recoil detection angle was 40° relative to the beam direction. The TOF–ERDA detector system consists of two timing gates, after which an ion-implanted semiconductor energy detector is placed. In the measurements both time-of-flight and energy of each recoil ion are measured in coincidence and the different masses can be separated. The measuring setup is described in detail in Ref. 14. The elemental energy spectra were converted to

<sup>a)</sup>Electronic mail: fal@uam.es

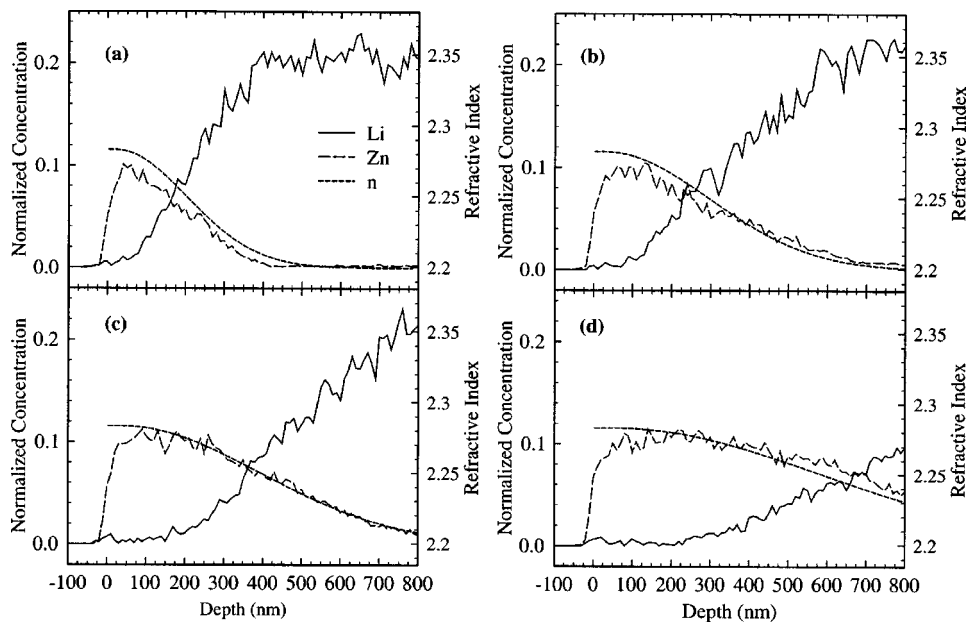


FIG. 1. Depth profiles for Li and Zn after the following Zn-diffusion treatments: (a) 550 °C, 30 min, (b) 600 °C, 30 min, (c) 550 °C, 2 h, (d) 600 °C, 2 h. The corresponding refractive index profile is included as a dotted line.

depth profiles using known measurement geometry, parametrized stopping powers,<sup>15</sup> and scattering cross sections. For each sample the total sum of the atomic concentration profiles was normalized to 1 at the surface.

It was checked that the energy spectra of all recoiled atoms were not appreciably modified during the experiments.

The depth profiles of all elements after the stage of Zn diffusion have been measured. Figure 1 shows the concentration profiles for the relevant, Li and Zn, elements. The depth profiles show that Li has been completely removed from the outermost layer of the sample (a few hundred nanometers) in correlation with a Zn-rich region. Below this layer the Zn concentration decreases whereas the Li profile recovers. In the whole investigated depth range, the sum  $\text{Li} + 2\text{Zn}$  remains approximately constant with depth at the value corresponding to the initial Li (and Nb) concentration. Therefore, it now becomes clear that the Zn-diffusion process is, in fact, an ion-exchange process ( $\text{Zn} \leftrightarrow 2\text{Li}$ ) from the vapor phase in the same way as H and Li are exchanged when  $\text{LiNbO}_3$  is immersed into a weak acid.<sup>16</sup> No oxygen leaks have been detected in our measurements. The stoichiometry data for the outermost layer can be satisfactorily fitted to a mixture  $\text{LiNbO}_3/\text{ZnNb}_2\text{O}_6$  with composition profiles shown in Fig. 2. The alternative hypothesis of a solid solution  $\text{Zn/LiNbO}_3$  does not describe the data and can, therefore, be discarded. Moreover, the inclusion of a third compound (ZnO) does not reduce the  $\chi^2$  per degree of freedom. Notice that the compound depth profiles are only shown up to 400 nm. Some inaccuracies in the input O and Nb depth profiles deteriorate somewhat the quality of the fit deeper inside the sample. The  $\text{ZnNb}_2\text{O}_6$  phase has been clearly observed in our x-ray experiments (see inset in Fig. 2), although the Bragg peaks are broad and relatively small in comparison with those found<sup>17</sup> after more aggressive treatments (20 h at 750 °C). The thickness of this Zn-rich layer increases as the temperature and/or duration of the treatment increase (100 nm at 550 °C and 30 min, 400 nm at 600 °C and 2 h). The region below the  $\text{ZnNb}_2\text{O}_6$  phase extends beyond the range of our ERDA technique and may correspond to a solid solution of Zn in  $\text{LiNbO}_3$  (a few microns

deep) according to secondary ion mass spectroscopy data.<sup>2</sup>

After that diffusion step the surface of the samples shows good quality without any sign of damage or pitting. Reflectivity experiments were performed with a polarized He-Ne laser operating at 633 nm, measuring the reflected light intensity at the prism-sample interface as a function of incidence angle. For the most heavily treated sample (2 h at 600 °C) the reflectivity spectra for extraordinary polarized light obtained using a high index prism coupling technique show two broad minima corresponding to refractive indices of 2.240 and 2.204. Since for  $\text{LiNbO}_3$ ,  $n_e = 2.2030$ , this result provides a clear indication of the formation of a high index surface layer after the Zn diffusion. The data can be well fitted with a graded Gaussian index profile yielding a maximum index of 2.280 and a depth of 750 nm. The data for the other treatments can also be fitted with the same type of profile and maximum index. The index profiles are shown in Fig. 1, together with the Li and Zn compositional profiles. The correlation between the optical and composition profiles is good.

After the annealing treatment at 900 °C the experimental Zn and Li profiles markedly change as illustrated in Fig. 3

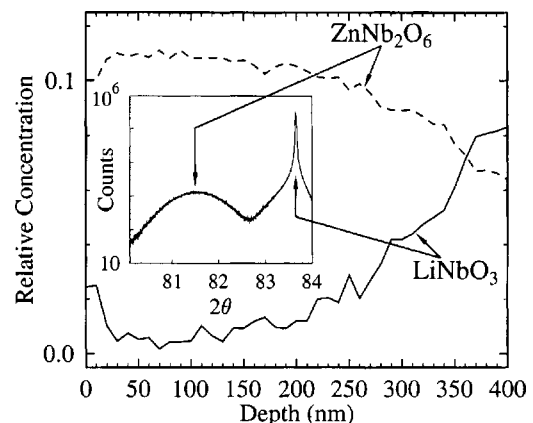


FIG. 2. Depth profiles showing the best fit to ERDA data for a Zn-diffused sample at 550 °C for 2 h. X-ray diffraction spectrum showing the presence of a  $\text{ZnNb}_2\text{O}_6$  phase is included in the inset.

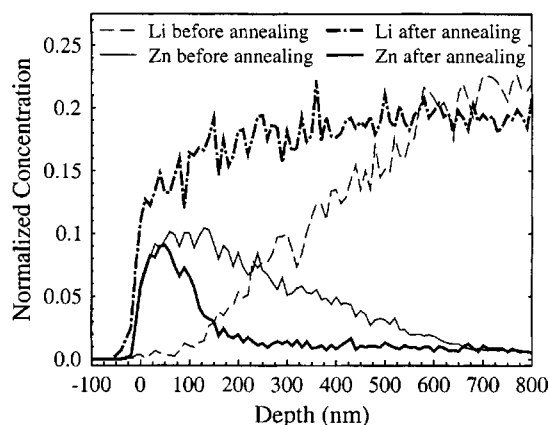


FIG. 3. Li and Zn depth profiles for a Zn-diffused waveguide (2 h, 550 °C) after an annealing treatment of 1 h at 900 °C. The profiles before annealing are included for comparison.

(the profiles before the Zn-diffusion step are included for comparison). The Li profile mostly recovers although it still experiences a decrease near the surface, particularly after more aggressive diffusion treatments. The Zn profile becomes narrower and concentrates at the surface in correlation with the Li deficiency. In fact, it can be easily checked that the concentrations of all elements assure local charge neutrality. From the concentration profiles the stoichiometry of the Zn-rich surface layer has been determined. The best description of the data is obtained with a mixture of  $\text{LiNbO}_3$  and  $\text{ZnO}$  phases and a small fraction of  $\text{ZnNb}_2\text{O}_6$  (see Fig. 4). All those phases present in the outermost layer had been previously identified in annealed waveguides after diffusion at 700 °C.<sup>13</sup> The thickness of the Zn rich layer varies from 100 to 400 nm, depending on the prior Zn-diffusion treatment.

Taking into account the earlier results the associated re-

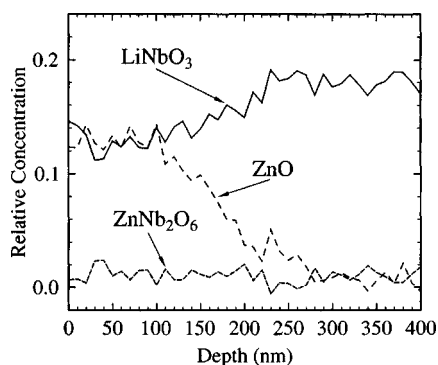


FIG. 4. Depth profiles showing the best fit to ERDA data for a Zn-diffused waveguide (2 h, 550 °C) after annealing at 900 °C for 1 h.

fractive index profile at the surface of the annealed waveguides can be simulated. In the outermost layer of  $\text{ZnO} + \text{LiNbO}_3$  of a few hundred nanometers, the extraordinary refractive index should be an average of the values for the two component phases (2.2 for  $\text{LiNbO}_3$  and 2.0 for  $\text{ZnO}$  at  $\lambda = 633$  nm), i.e., around 2.1. This outermost thin layer with a lower refractive index than  $\text{LiNbO}_3$  accounts for the difficulties found to couple light into the waveguide by the prism method. Below that layer, i.e., beyond the capabilities of the ERDA technique a graded refractive index profile is found, extending to a depth of a few microns, and corresponding to Zn-doped  $\text{LiNbO}_3$ .<sup>18</sup>

In conclusion, ERDA-TOF experiments carried out with 55 MeV  $^{127}\text{I}$  ions have provided very detailed and quantitative information on the composition and depth stacking of the surface layers (<500 nm thick) that are formed during the Zn diffusion and subsequent high temperature annealing. The composition profiles of the layers are in agreement with the refractive index and waveguiding behavior.

This work is dedicated to Professor Domingo González, from the University of Zaragoza, on the occasion of his retirement.

- <sup>1</sup>R. C. Alferness, IEEE J. Quantum Electron. **QE-17**, 946 (1981).
- <sup>2</sup>R. Nevado, F. Cussó, G. Lifante, F. Caccavale, C. Sada, and F. Segato, J. Appl. Phys. **88**, 6183 (2000).
- <sup>3</sup>W. W. Young, R. S. Feigelson, M. M. Fejer, M. J. F. Digonnet, and H. J. Shaw, Opt. Lett. **16**, 995 (1991).
- <sup>4</sup>T. Kawaguchi, K. Mizuuchi, T. Yoshino, M. Imaeda, K. Yamamoto, and T. Fukuda, J. Cryst. Growth **203**, 173 (1999).
- <sup>5</sup>H. Li, G. Xu, G. Hu, and X. Wang, Cryst. Res. Technol. **29**, 693 (1994).
- <sup>6</sup>T. Volk, N. Rubinina, and M. Wohlecke, J. Opt. Soc. Am. B **11**, 1681 (1994).
- <sup>7</sup>F. Abdi, M. Aillerie, M. Fontana, P. Boulon, T. Volk, B. Maximov, S. Sulyanov, N. Rubinina, and M. Wohlecke, Appl. Phys. B: Lasers Opt. **68**, 795 (1999).
- <sup>8</sup>R. Nevado, E. Cantelar, G. Lifante, and F. Cussó, Jpn. J. Appl. Phys., Part 2 **39**, L488 (2000).
- <sup>9</sup>J. Ichikawa, S. Uda, K. Shimamura, and T. Fukuda, Appl. Phys. Lett. **76**, 1498 (2000).
- <sup>10</sup>C. Huang and L. M. McCaughan, Electron. Lett. **33**, 1639 (1997).
- <sup>11</sup>R. Nevado and G. Lifante, J. Opt. Soc. Am. A **16**, 2574 (1999).
- <sup>12</sup>H. J. Whitlow, in *Proceedings of High Energy and Heavy Ion Beams in Materials Analysis, Albuquerque, New Mexico, 1989*, edited by J. R. Tesmer, C. J. Maggiore, M. Nastasi, and J. C. Barbour (Materials Research Society, Pittsburgh, PA, 1990), p. 243.
- <sup>13</sup>F. Schiller, B. Herreros, and G. Lifante, J. Opt. Soc. Am. A **14**, 425 (1997).
- <sup>14</sup>J. Jokinen, P. Haussalo, P. Tikkanen, A. Kuronen, T. Ahlgren, and K. Norlund, Nucl. Instrum. Methods Phys. Res. B **119**, 533 (1996).
- <sup>15</sup>J. F. Ziegler, J. P. Bierzak, and U. Littmark, *The Stopping and Range of Ions in Matter* (Pergamon, New York, 1985).
- <sup>16</sup>J. M. Cabrera, J. Olivares, M. Carrascosa, J. Rams, R. Müller, and E. Diéguez, Adv. Phys. **45**, 349 (1996).
- <sup>17</sup>V. A. Fedorov, Yu N. Korkishko, F. Vereda, G. Lifante, and F. Cussó, J. Cryst. Growth **194**, 94 (1998).
- <sup>18</sup>R. Nevado and G. Lifante, Mater. Sci. Eng. **72**, 725 (2001).